AN ESS LINAC COLLIMATION STUDY

R. Miyamoto*, ESS, Lund, Sweden

Abstract

The European Spallation Source is planned in Lund, Sweden, and will be a neutron source based on a proton linac with an unprecedented 5 MW beam power. Mitigation of beam losses is the most crucial challenge in beam physics for such a high power proton linac and collimation systems are planned in sections of the medium and high energy beam transport (MEBT and HEBT). A preliminary study of the collimation systems was presented in the previous time of this workshop but the linac design went through a significant revise since then. The system to expand the beam for the target, located in the HEBT, was changed from one based on nonlinear magnets to a raster system and this change particularly had a significant impact on the demand on the collimation systems. This paper presents an updated beam dynamics study of the collimation systems for the present layout of the ESS Linac.

INTRODUCTION

The European Spallation Source (ESS) will be a neutron source in Lund, Sweden, based on a proton linac with an unprecedented 5 MW beam power [1]. Figure 1 shows a layout of the ESS Linac and Table 1 summarizes its high level parameters. The linac consists of normal conducting accelerating structures, sections of superconducting cavities, and low, medium, and high energy beam transports (LEBT, MEBT, and HEBT). The normal conducting accelerating structures include an ion source (IS), radio frequency quadrupole (RFQ), and drift tube linac (DTL). The ESS Linac uses three types of superconducting cavities: spoke, medium-β elliptical, and high-β elliptical cavities. The sections of the superconducting cavities are also referred to as the Superconducting (SC) Linac as a whole.

For a high power machine such as the ESS Linac, minimization of beam losses is crucial to allow hands-on maintenance as well as to protect machine components and imposes difficult challenges on the design and machine tuning. Based on the experience of SNS [2], a system of beam scrapers is planned for the MEBT to improve beam quality in an early stage of the linac and thus to lower the risk of the beam losses as possible. Beam dynamics simulations indicated its use for the ESS Linac too [3–5] but its effect throughout the entire linac, taking into account various errors, has not been thoroughly studied yet. Collimation systems have been also considered for the HEBT where the beam power is the highest 5 MW [3, 6]. However, since the design revision in 2013 [7], the system to expand the beam for the target has been switched from one based on nonlinear magnets [8] to the other using raster magnet [9] and the present system is much less sensitive to the transverse beam halo. This

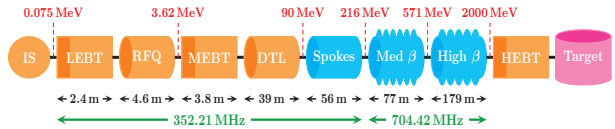

Figure 1: Layout of the ESS Linac. Blue color indicates a section of superconducting cavities.

Table 1: High Level Parameters of the ESS Linac

Parameter	Unit	Value
Average beam power	MW	5
Maximum beam energy	GeV	2
Peak beam current	mA	62.5
Beam pulse length	ms	2.86
Beam pulse repetition rate	Hz	14
Duty cycle	%	4
RF frequency	MHz	352.21/704.42

led present reconsideration of the collimation systems in the HEBT. An input to make the decision is quality of the beam entering the HEBT. Thus, on this occasion, impact of the MEBT scrapers on the beam quality and losses throughout the entire linac, especially the later part of the linac, is studied in detail in this paper

CONDITIONS FOR SIMULATIONS

This section discusses conditions of the simulations in the following sections. Throughout the paper, the lattice in [1] is used. All the simulations are done by tracking the pre-calculated RFQ output beam from the MEBT entrance with the TraceWin code [10]. Space-charge force is calculated with the 3D PICNIC routine [11] with a step size of 15 per [(relativistic-β) $\times$ (wavelength)] and a mesh of $10 \times 10 \times 10$.

RFQ Output

The output beam from the RFQ is simulated with the Toutatis code [12] by assuming 2D Gaussian distribution with a normalized emittance of 0.25 π mm mrad at its entrance. The number of macro-particles is either 1×10^5, 1×10^6, or 1×10^7, depending on a type of a study. Table 2 summarizes the parameters of the simulated output beam.

Table 2: RMS Normalized Emittances (ϵ) and Courant-Snyder Parameters (β and α) of the RFQ Output Beam

Plane	ϵ [π mm mrad]	β [m]	α
x	0.253	0.210	−0.052
y	0.252	0.371	−0.310
z	0.361	0.926	−0.481

* ryoichi.miyamoto@esss.se

ISBN 978-3-95450-173-1

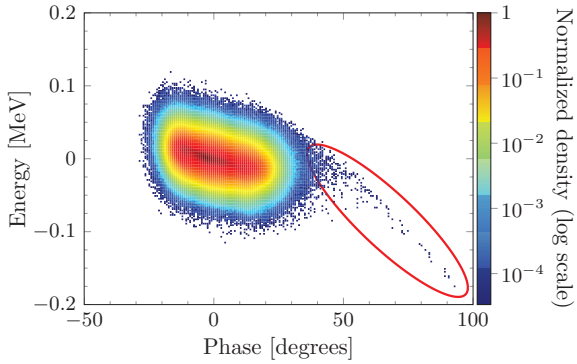

Figure 2: RFQ output distribution on the longitudinal phase space. The longitudinal tail is marked with a red ellipse.

Figure 2 shows the RFQ output distribution on the longitudinal phase space (1×10^7 macro-particles case). An RFQ output beam often has a structure referred to as *longitudinal tail* (the part marked with an ellipse), and these off-momentum particles are of concern for beam losses.

MEBT Scrapers

Figure 3 shows the present MEBT layout together with beam envelopes and apertures, where three locations with tight apertures at 0.85, 2.19, and 3.39 m correspond to the scrapers. The scraper system at each location has two blades per plane and four in total for both plane. At present, the scraper is being designed so that each blade can absorb ~12 W or ~0.14% of the beam, corresponding a 3σ distance to the beam center for a Gaussian beam. This specification is based on the previous beam simulations [3, 4] and its engineering feasibility is supported by [3, 13]. The set of three scrapers provides an efficient cleaning in case the beam out of the RFQ has transverse halos and also improves quality of the nominal beam [4].

The IS and LEBT have transient times during turning on and off and bunches from these times, positioned at the head and tail of a macro-pulse, are likely to have wrong parameters. One of main functions of the MEBT is to house a fast chopper of an electric deflector to remove these bunches.

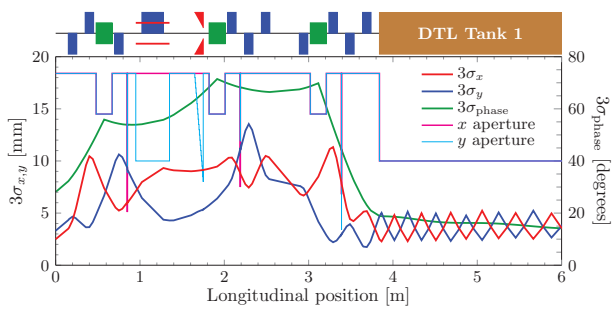

Figure 3: MEBT layout, 3σ beam envelopes, and apertures. On the top, blue boxes above (below) the line represent focusing (defocusing) quadrupoles, green boxes buncher cavities, and red lines and triangles a chopper and its dump. Three locations with tight apertures correspond to the scrapers.

Table 3: Lattice Error Tolerances (the distributions are uniform with the listed amplitudes. For DTL, the cavity error is random for each accelerating gap whereas the tank error is a systematic and common for all the gaps in one tank)

Sect	Elem	Mode	$\delta x, \delta y$ mm	$\delta\theta_x, \delta\theta_y$ deg	$\delta\theta_z$ deg	$\delta E, \delta B$ %	$\delta\phi$ deg
MEBT	Quad	Stat	0.2	0	0.06	0.5	—
	Cav	Stat	0.5	0.115	—	1	1
	Cav	Dyn	0	0	—	0.2	0.2
DTL	Quad	Stat	0.1	0.5	0.2	0.5	—
	Cav	Stat	0	0	—	1	0.5
	Tank	Stat	0	0	—	1	1
	Tank	Dyn	0	0	—	0.2	0.2
SC	Quad	Stat	0.2	0	0.06	0.5	—
	Cav	Stat	1.5	0.129	—	1	1
	Cav	Dyn	0	0	—	0.1	0.1
HEBT	Quad	Stat	0.2	0	0.06	0.5	—
	Bend	Stat	0.2	0	0.06	0.05	—

The rise time of the fast chopper is specified as ~10 ns at present and, given the bunch space is 2.84 ns, a few bunches receive a partial voltage. These *partially-chopped* bunches could have large trajectory excursions and raise a concern, but the scrapers also improve the situation of the beam losses due to these bunches [5].

Input Beam and Lattice Errors

To estimate the situation of the beam loss, the effects of all possible errors must be taken into account. A campaign of identifying the tolerances of lattice element errors was conducted this year based on a criteria to limit an emittance growth of each plane per section to ~10% [14, 15]. Table 3 lists the found tolerance values where the distribution of each error type is uniform with an amplitude of the given value. Table 4 lists the expected errors in the RFQ output when the tolerance values of the lattice element errors are applied to the RFQ. In statistical studies of the following sections, the error values listed in these two tables are used.

Table 4: Errors in the RFQ Output Beams (a uniform distribution with the listed amplitude is assumed for each error in a simulation. The symbol $M_{x,y,z}$ is the mismatch factor)

Parameter	Unit	Value
$\delta x, \delta y$	mm	0.3
$\delta x', \delta y'$	mrad	1
$\delta\phi$	degrees	0
δW	keV	10
$\delta\epsilon_x, \delta\epsilon_y, \delta\epsilon_z$	%	5
M_x, M_y, M_z	%	5
δI	mA	0.625

ISBN 978-3-95450-173-1

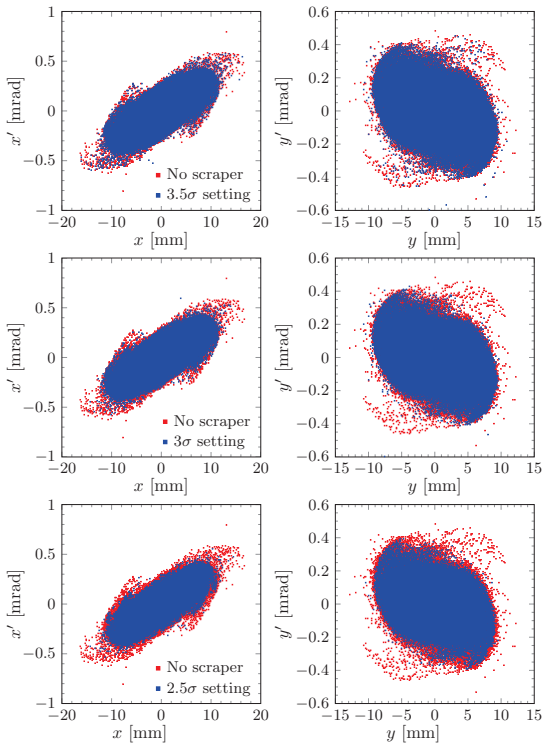

Figure 4: Transverse phase space distributions at the HEBT entrance for the scraper positions of 3.5σ, 3σ, and 2.5σ.

FORWARD TRACKING

The simplest way to study the effect of the MEBT scrapers is to track the beam with and without the scrapers and to observe the distribution at locations of interest. Figure 4 compares the distributions on the transverse phase spaces at the HEBT entrance (1×10^7 macro-particles) for the cases when each scraper blade is positioned so as to absorb ~2.1 W (0.02%), ~12 W (0.14%), and ~56 W (0.621%). These correspond to the 3.5σ, 3σ, and 2.5σ distances to the beam center if the distribution is a Gaussian. The distribution in red represents the case of no scraper as a reference. The improvement for the 3.5σ case is hard to see but the 3σ and 2.5σ cases are showing a clear cleaning effect of the outermost particles, particularly for the vertical plane.

Figure 5 shows the histograms of the radial distributions on the normalized phase spaces for the distributions of Fig. 4. Though the cleaning effects of the 3σ and 2.5σ cases are clear, the outermost particles extend as far as 10σ toward the end of the linac and the scrapers can remove only particles beyond 8σ. Figure 6 shows the histograms of the radial distributions on the normalized phase space along several locations in the linac, comparing the cases with and without the scrapers. The extent of the outermost particles gradually increases along the linac. The scrapers could reduce this extent but cannot maintain it to the level of the MEBT exit.

BACKWARD TRACKING

To understand the situation of the halo better, this section tries another type of analysis. In Figure 7, the particles

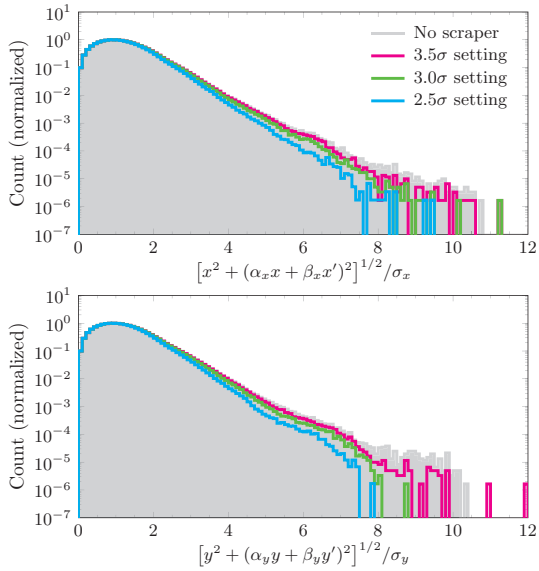

Figure 5: Radial distributions on the normalized phase spaces for the distributions of Fig. 4.

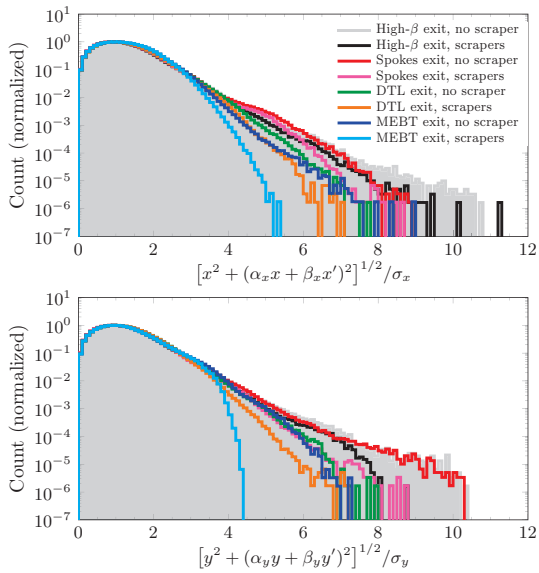

Figure 6: Evolution of the distribution along the linac with and without the scrapers (3σ case).

beyond 4σ on the normalized phase spaces of the transverse planes are defined as halo (illustrated on the first row) and their phase space positions are observed at several upstream locations. The part in magenta represents the core which ends up within 4σ at the HEBT entrance. This analysis is memory consuming and only 1×10^6 macro-particle are used. As seen in the figure, a significant fraction of the halo particles is originally well within the core in an early part of the linac but gradually diffused out along the linac. Please note this is due to the strong space-charge force and do not occur for the case of a weak current. Figure 8 shows the histograms of the radial distribution on the normalized phase spaces for the distributions of Fig. 7. The figure again shows the trend of particles within the core in an early part of the

ISBN 978-3-95450-173-1

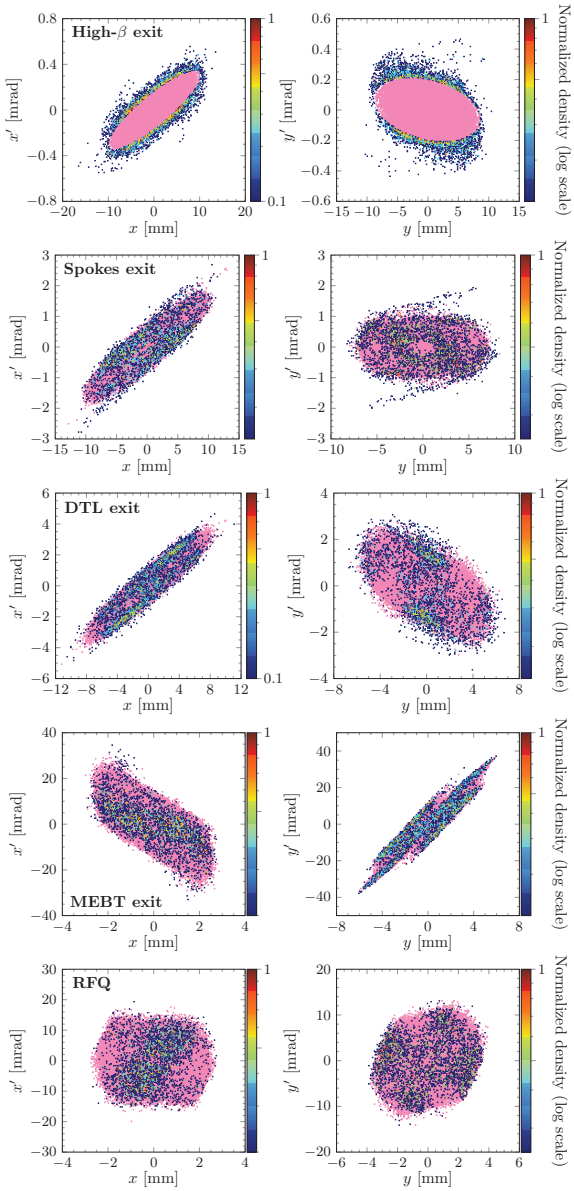

Figure 7: Distributions of the halo particles (particles beyond 4σ at the HEBT entrance) at upstream locations.

linac ending up being the halo toward the end. It also shows that a large fraction of this diffusive process occur after the section of spoke cavities. This result indicates there is also a fundamental limitation in the cleaning with the MEBT scrapers.

BEAM LOSS

Beam Loss with and without Errors

This section discusses the beam losses in the ESS Linac and the impact of the MEBT scrapers on it. Before taking into account the errors, Figure 9 shows the beam losses in the case of no lattice error when 1×10^7 macro-particles shown in Fig. 2 are tracked. The location near the upstream vertical bend in the HEBT and the DTL are typical places of the beam losses in the ESS Linac. Please note that the most

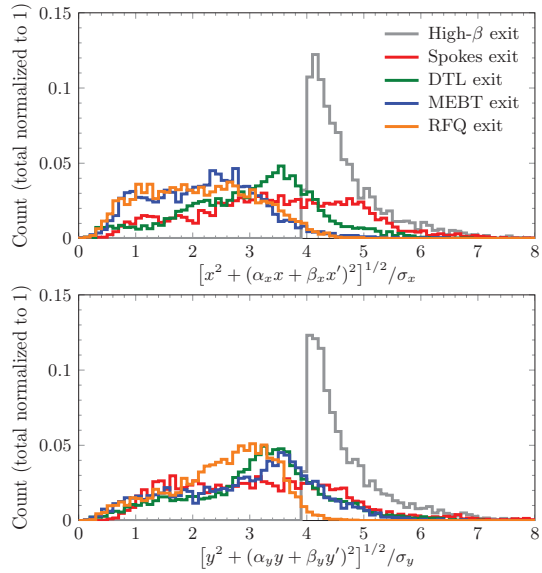

Figure 8: Radial distributions on the normalized phase spaces for the halo particles of Fig. 7.

of the lost particles are originally in the longitudinal tail and, because of that, the scrapers do not make a big difference.

Figure 10 shows the losses when the errors in Tables 3 and 4 are included. In the calculation, 1×10^5 macro-particles are tracked in 1000 linacs of different random seeds. The *confidence level loss* of 90% and 99% are the maximum loss at each location after excluding the largest 10% and 1% cases. Please note that the trajectory error is corrected with steerer dipoles based on simulated beam position monitors with anticipated finite accuracy. When the lattice errors are introduced, the scrapers are placed so that the 99% confidence level loss per blade does not exceed 12 W, giving slightly less cleaning than the 3σ setting for the no error

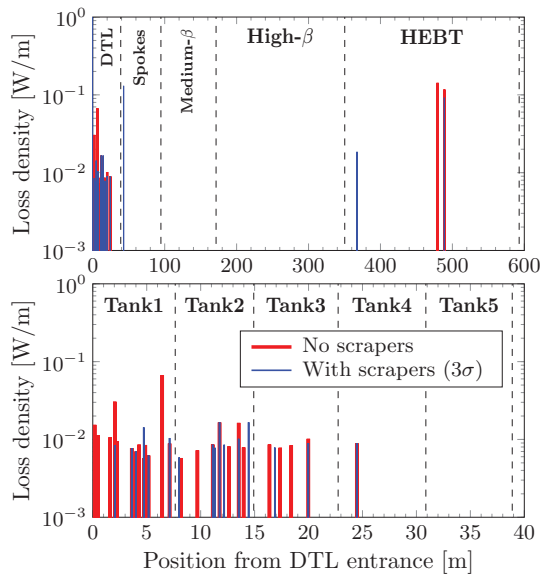

Figure 9: Beam losses due to 1×10^7 macro-particles in case of no lattice error. The bottom is a close-up of the DTL.

ISBN 978-3-95450-173-1

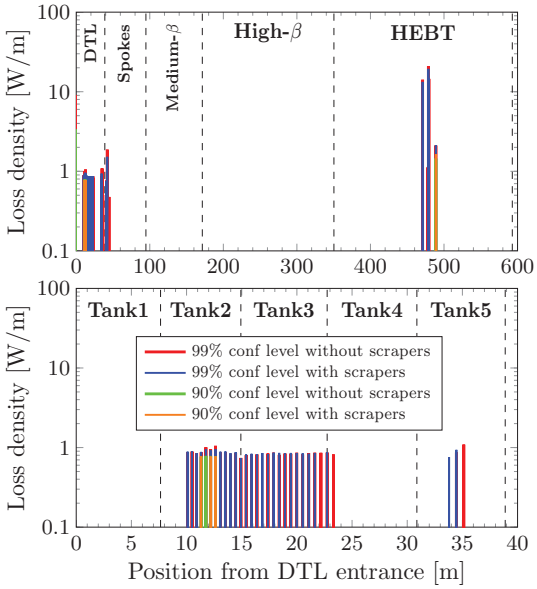

Figure 10: Confidence level losses when the errors in Tables 3 and 4 are taken into account.

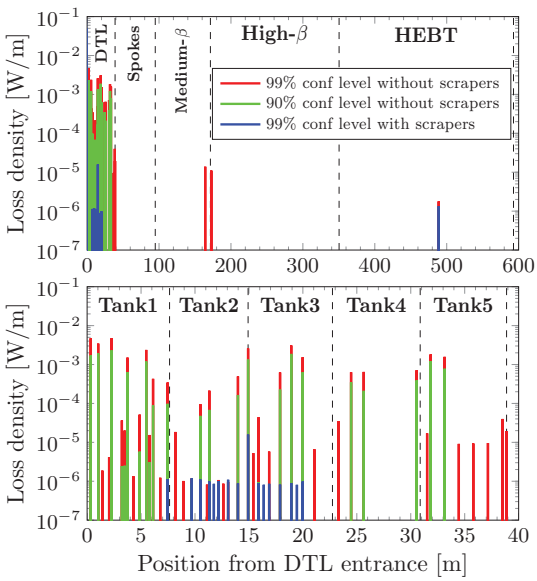

Figure 11: Confidence level losses due to a partially-chopped bunch for the case of 1.5 kV chopper voltage (nominal 4 kV).

case. As the case of no error in Fig. 9, the scrapers do not make a big difference, indicating that the beam loss is due to dynamics of longitudinal plane even with the lattice errors and the linac has a wide enough aperture for the given error.

Beam Loss Due to Partially-chopped Bunches

As discussed in Section *MEBT Scrapers*, the partially-chopped bunches cause some beam losses. Because the result in [5] did not include the HEBT, the simulation is repeated here. Both the chopper and lattice errors introduce trajectory excursions but the latter one should be compensated as mentioned above. However, due to the limitations in the setup of the simulation, this was not done properly and the result in [5] included the excursions from both sources, thus providing unnecessary pessimistic result. In addition to include the HEBT, this limitation was also solved in the following result. Figure 11 shows the confidence level losses due to one partially-chopped bunch when 1×10^5 macro-particles are tracked in 500 linacs. The previous study showed that the beam loss situation is worst when the chopper voltage is around 1.5 kV (the nominal is 4 kV) [5] so the 1.5 kV is applied as a representative case. The lattice errors in Table 3 are again applied, but the input beam error of Table 4 and the lattice errors up to the chopper dump in the MEBT are not applied to keep the condition up to the dump the same. The loss in the HEBT is only $\sim 1 \times 10^{-5}$ W/m level with 99% confidence even without the scrapers and is not a concern. As the previous study indicated [5], the scrapers make a significant reduction of the losses, particularly in the DTL, since these losses are due to the dynamics on the transverse plane (trajectory excursion).

CONCLUSIONS

The impact of the MEBT scrapers on the beam quality and losses throughout the ESS Linac is studied in detail. The cleaning effect of the scrapers are evident, but there are fundamental limitations and the scrapers can only prevent the outermost particles from exceeding $\sim 8\sigma$ toward the end of the linac. The beam loss in the ESS Linac is likely caused by dynamics on the longitudinal plane and thus the scrapers look to have no significant effect on the beam losses, except those caused by the partially-chopped bunches.

ACKNOWLEDGMENTS

The author would like to thank to M. Eshraqi, R. De Prisco, E. Sargsyan, and H. D. Thomsen for providing the data of the beam distribution and lattice and also I. Bustinduy, B. Cheymol, H. Danared, and A. Ponton for useful discussions.

REFERENCES

[1] M. Eshraqi et al., in Proc. of IPAC'14, THPME043.
[2] M. A. Plum, in Proc. of HB'12, TUO3C04.
[3] R. Miyamoto et al., in Proc. of HB'12, WEO3A02.
[4] R. Miyamoto et al., in Proc. of IPAC'14, THPME045.
[5] R. Miyamoto et al., in Proc. of LINAC'14, MOPP039.
[6] H. D. Thomsen and S. P. Møller, in Proc. of IPAC'12, MOPPD072.
[7] M. Eshraqi et al., in Proc. of IPAC'13, THPWO072.
[8] A. I. S. Holm et al., in Proc. of IPAC'12, MOPPD049.
[9] H. D. Thomsen and S. P. Møller, in Proc. of IPAC'14, WEPRO072.
[10] R. Duperrier et al., in Proc. of ICCS'02, p. 411.
[11] N. Pichoff et al., in Proc. of Linac'98, MO4042.
[12] R. Duperrier, PRST-AB **3**, 124201 (2000).
[13] I. Bustinduy et at., in Proc. of HB'14, TUO1AB04, to be published.
[14] M. Eshraqi et al., in Proc. of IPAC'14, THPME044.
[15] H. D. Thomsen and S. P. Møller, in Proc. of IPAC'14, WEPRO074.

ISBN 978-3-95450-173-1